

Theoretical study on Brillouin fiber laser sensor based on white light cavity

Omer Kotlicki,¹ Jacob Scheuer,^{1,2,*} and M.S. Shahriar^{2,3}

¹ School of Electrical Engineering Tel Aviv University, Ramat Aviv, Tel-Aviv 69978, Israel

² Departments of Electrical Engineering and Computer Science, Northwestern University, Illinois 60208, USA

³ Departments of Physics and Astronomy, Northwestern University, Illinois 60208, USA

*kobys@eng.tau.ac.il

www.eng.tau.ac.il/~kobys/

Abstract: We present and theoretically study a superluminal fiber laser based super-sensor employing Brillouin gain. The white light cavity condition is attained by introducing a phase shift component comprising an additional ring or Fabry-Perot cavity into the main cavity. By adjusting the parameters of the laser cavity and those of the phase component it is possible to attain sensitivity enhancement of many orders of magnitude compared to that of conventional laser sensors. The tradeoffs between the attainable sensitivity enhancement, the cavity dimensions and the impact of the cavity roundtrip loss are studied in details, providing a set of design rules for the optimization of the super-sensor.

©2012 Optical Society of America

OCIS codes: (280.3420) Laser sensors; (290.5830) Scattering, Brillouin.

References and links

1. P. Hariharan, *Basics of Interferometry*, 2nd ed (Academic Press, 2006).
2. G. Gauglitz, "Direct optical sensors: principles and selected applications," *Anal. Bioanal. Chem.* **381**(1), 141–155 (2005).
3. B. J. Meers, "Recycling in laser-interferometric gravitational-wave detectors," *Phys. Rev. D Part. Fields* **38**(8), 2317–2326 (1988).
4. G. Heinzel, K. A. Strain, J. Mizuno, K. D. Skeldon, B. Willke, W. Winkler, R. Schilling, A. Rudiger, and K. Danzmann, "Experimental demonstration of a suspended dual recycling interferometer for gravitational wave detection," *Phys. Rev. Lett.* **81**(25), 5493–5496 (1998).
5. M. B. Gray, A. J. Stevenson, H.-A. Bachor, and D. E. McClelland, "Broadband and tuned signal recycling with a simple Michelson interferometer," *Appl. Opt.* **37**(25), 5886–5893 (1998).
6. B. J. Meers, "The frequency response of interferometric gravitational wave detectors," *Phys. Lett. A* **142**(8-9), 465–470 (1989).
7. P. Lambeck, "Integrated optical sensors for the chemical domain," *Meas. Sci. Technol.* **17**(8), R93–R116 (2006).
8. A. Leung, P. M. Shankar, and R. Mutharasan, "A review of fiber-optic biosensors," *Sens. Actuators B Chem.* **125**(2), 688–703 (2007).
9. R. Ulrich, "Fiber-optic rotation sensing with low drift," *Opt. Lett.* **5**(5), 173–175 (1980).
10. R. E. Meyer, S. Ezekiel, D. W. Stowe, and V. J. Tekippe, "Passive fiber-optic ring resonator for rotation sensing," *Opt. Lett.* **8**(12), 644–646 (1983).
11. A. Leneff, T. D. Hammond, E. T. Smith, M. S. Chapman, R. A. Rubenstein, and D. E. Pritchard, "Rotation sensing with an atom interferometer," *Phys. Rev. Lett.* **78**(5), 760–763 (1997).
12. G. S. Pati, M. Salit, K. Salit, and M. S. Shahriar, "Demonstration of a tunable-bandwidth white-light interferometer using anomalous dispersion in atomic vapor," *Phys. Rev. Lett.* **99**(13), 133601 (2007).
13. M. S. Shahriar, G. S. Pati, R. Tripathi, V. Gopal, M. Messall, and K. Salit, "Ultrahigh enhancement in absolute and relative rotation sensing using fast and slow light," *Phys. Rev. A* **75**(5), 053807 (2007).
14. H. N. Yum, M. Salit, J. Yablon, K. Salit, Y. Wang, and M. S. Shahriar, "Superluminal ring laser for hypersensitive sensing," *Opt. Express* **18**(17), 17658–17665 (2010).
15. J. Schaar, H. Yum, and M. S. Shahriar, "Theoretical Description and Design of a Fast-Light Enhanced Helium-Neon Ring-Laser Gyroscope," *Proc. SPIE 7949, Advances in Slow and Fast Light IV*, 794914 (2011).
16. S. Wise, G. Mueller, D. Reitze, D. B. Tanner, and B. F. Whiting, "Linewidth-broadened Fabry-Perot cavities within future gravitational wave detectors," *Class. Quantum Gravity* **21**(5), S1031–S1036 (2004).
17. S. Wise, V. Quetschke, A. J. Deshpande, G. Mueller, D. H. Reitze, D. B. Tanner, B. F. Whiting, Y. Chen, A. Tünnermann, E. Kley, and T. Clausnitzer, "Phase effects in the diffraction of light: beyond the grating equation," *Phys. Rev. Lett.* **95**(1), 013901 (2005).

18. A. Kobayakov, M. Sauer, and D. Chowdhury, "Stimulated Brillouin scattering in optical fibers," *Adv. Opt. Photon.* **2**(1), 1–59 (2010).
19. M. O. Scully and W. E. Lamb, *Laser Physics* (Westview Press, Boulder, CO, 1974).
20. T. A. Dorschner, H. A. Haus, M. Holz, I. W. Smith, and H. Statz, "Laser gyro at quantum limit," *IEEE J. Quantum Electron.* **16**(12), 1376–1379 (1980).
21. J. D. Cresser, W. H. Louisell, P. Meystre, W. Schleich, and M. O. Scully, "Quantum noise in ring laser gyros. I. Theoretical formulation of the problem," *Phys. Rev. A* **25**(4), 2214–2225 (1982).
22. B. T. King, "Application of superresolution techniques to ring laser gyroscopes: exploring the quantum limit," *Appl. Opt.* **39**(33), 6151–6157 (2000).
23. S. Huang, L. Thevenaz, K. Toyama, B. Y. Kim, and H. J. Shaw, "Optical Kerr-effect in fiber-optic Brillouin ring laser gyroscopes," *IEEE Photon. Technol. Lett.* **5**(3), 365–367 (1993).

1. Introduction

Optical interferometers and resonators constitute among the most precise physical measurement approaches, rendering them key-components for numerous and diverse research fields [1,2]. The applications for such devices range from fundamental scientific studies requiring ultra-precision measurements [2–6] to biochemical sensing [7,8], navigation [9–11] and more. Interferometers and resonators utilize the ability to detect and measure accurately phase shifts that are induced by small changes in the optical path of the light in the device. While the physical causes for the optical path changes could be diverse (temperature, displacement, rotation, chemical effect, etc.), the detection mechanisms are similar. An interferometer makes use of interference between light passing through a disturbed and an undisturbed optical path to detect and measure the level of perturbation. A resonator utilizes the disturbance induced shift of its resonance frequency to quantify the disturbance.

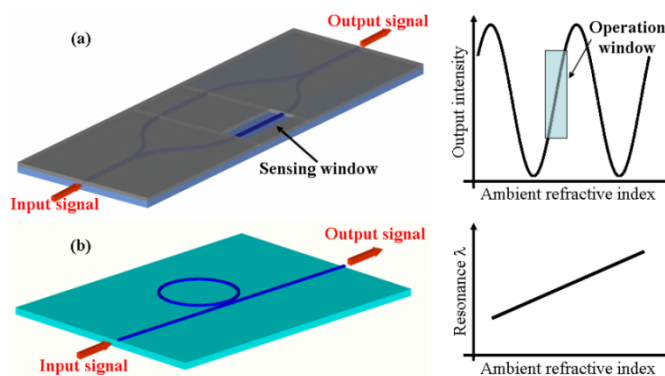


Fig. 1. Interferometric (a) and resonator-based (b) optical measurement schemes.

We emphasize that although we clearly distinguish interferometers from resonators (two-wave vs. multi-wave interference) the devices are based on similar physics. The origin for the resonance shift in a disturbed resonator is the spatio-temporal interference of the light in the cavity with itself. The reason for the clear distinction is that a resonator may include an active amplifying section and become eventually a self-oscillating device (laser). To date, most the interferometers and resonators employed for precise measurements and sensing are designed to exhibit linear response, i.e. the measured output depends linearly on the modifying quantity [1]. Figure 1 depicts representative interferometric and resonator-based optical sensing schemes. Although the specific illustrations concern refractive index measurements, similar architectures can be adapted for other types of measurements and sensing.

In the interferometric scheme, Fig. 1(a), changes in the ambient refractive index modify the phase accumulated by the wave propagating in the exposed arm, resulting in intensity changes in the output signal, or in a wavelength-interrogation mode we measure frequency shifts in dips or peaks. In the resonator-based scheme, Fig. 1(b), the ambient index modifies the resonance wavelength of the cavity. In both cases, the important parameter is the slope of

the measured signal as a function of the measured quantity – the steeper the slope the higher the sensitivity and, hence, the accuracy of the measurement.

Here, we focus on the white light cavity (WLC) effect [12–17] as a technique for substantially enhancing the sensitivity of an optical resonator based sensor to changes in the parameters of the environment, compared to a conventional laser sensor. In particular, we present and analyze a Brillouin based fiber laser implementation of a WLC ultra-sensitive sensor. Compared to the concepts presented previously [14,15], the novelty here is in all-fiber implementation of the WLC enhanced sensor, and the use of Brillouin gain for realizing the ring laser necessary for this implementation. This approach introduces new architectural and performance optimization issues that were not addressed in previous work. Furthermore, the all-fiber approach makes this device potentially simpler to realize, and opens up areas of application (such as strain sensing) that are not accessible in the systems proposed previously.

It is important to understand that the enhanced sensitivity provided by the WLC (see section 2 below) does not lead to a corresponding improvement in the minimum measurable phase shift. This is because the accuracy of measuring the resonance wavelength depends on the cavity linewidth which is broadened by the WLC effect. In fact, the WLC is broadened by a factor that essentially matches the enhancement in sensitivity [13]. In order to avoid this problem it is necessary to use an active cavity (i.e. a laser). The laser linewidth is determined by several mechanisms and is generally substantially narrower than that of the cold cavity, thus allowing one to exploit the sensitivity enhancement of the WLC concept.

2. White light cavity sensor

For illustration purposes, consider the white-light Fabry-Perot cavity depicted in Fig. 2. The WLC structure [16,17] consists of a conventional resonator incorporating at least one intra-cavity anomalous dispersive element. Figure 2 illustrates a generic optical cavity with length $L/2$, incorporating a dispersive section of length $l/2$. For a given frequency ω_0 , the phase shift accumulated in a single roundtrip is given by:

$$\Delta\phi(\omega_0) = \frac{\omega_0}{c_0} [(L-l) + n_l(\omega_0) \cdot l] \quad (1)$$

where n_l is the index of refraction for the dispersive section. For simplicity it was assumed that the refractive index of the non-dispersive section is unity. On resonance, the total phase accumulated in a single roundtrip must be an integer number of 2π , i.e. $\Delta\phi(\omega_{res}) = 2\pi m$. In order to achieve the WLC condition we need $\Delta\phi$ to remain $2\pi m$ regardless the frequency, at least within a certain vicinity of ω_{res} :

$$\Delta\phi(\omega_{res} + \Delta\omega) = \frac{(\omega_{res} + \Delta\omega)}{c_0} [(L-l) + n_l(\omega_{res} + \Delta\omega) \cdot l] = 2\pi m \quad (2)$$

Expanding Eq. (2) and subtracting Eq. (1) from it, keeping only the leading terms in $\Delta\omega$, yields the negative slope necessary for the WLC condition:

$$n_l(\omega_{res}) + \omega_{res} \left. \frac{dn_l}{d\omega} \right|_{\omega_{res}} = n_g(\omega_{res}) = 1 - L/l \quad (3)$$

where n_g is the group index of the section l at ω_{res} and the dispersion relation of that section close to resonance was expanded to the first order in $\Delta\omega$. Note, that Eq. (3) clearly indicate that n_g must be smaller than one or even negative in order to satisfy the WLC condition, which means that it must have anomalous dispersion.

To extend the condition Eq. (3) to a general case of WLC we write Eq. (2) in a more general form where the “fast-light” section in the cavity is assumed to add a frequency

dependent phase shift and it is assumed that the rest of the cavity consists of a (positive) dispersive medium. Thus, our generic superluminal laser includes an additional phase element which introduces anomalous phase shift to the cavity. This phase shift ideally compensates the normal dispersion of the cavity such that:

$$\Delta\varphi(\omega_{res} + \Delta\omega) = \frac{(\omega_{res} + \Delta\omega)}{c_0} n_p(\omega_{res} + \Delta\omega) \cdot L' + \theta(\omega_{res} + \Delta\omega) = 2\pi m \quad (4)$$

where ω_{res} is a resonance frequency of the cavity, n_p is the refractive index of the normal-dispersion medium inside the cavity, L' is the cavity length, θ is the phase response of the phase element, m is an integer, and $\Delta\omega$ is an arbitrary frequency shift. Expanding Eq. (4) to first order in $\Delta\omega$, i.e. $\theta(\omega_{res} + \Delta\omega) \approx \theta(\omega_{res}) + d\theta/d\omega \cdot \Delta\omega$ and $n_p(\omega_{res} + \Delta\omega) \approx n_p(\omega_{res}) + dn_p/d\omega \cdot \Delta\omega$ yields:

$$\left. \frac{d\theta}{d\omega} \right|_{\omega_{res}} = -\frac{L'}{c_0} \left[n_p(\omega_{res}) + \omega_{res} \frac{dn_p}{d\omega} \right] = -\frac{L'}{c_0} n_{pg} = -2\pi / \Delta\omega_{FSR} \quad (5)$$

where n_{pg} is the group index of the positive dispersion medium and $\Delta\omega_{FSR}$ is the free spectral range of the cavity without the fast-light phase section. Equation (5) provides a general condition for the phase shift needed to attain the WLC condition.

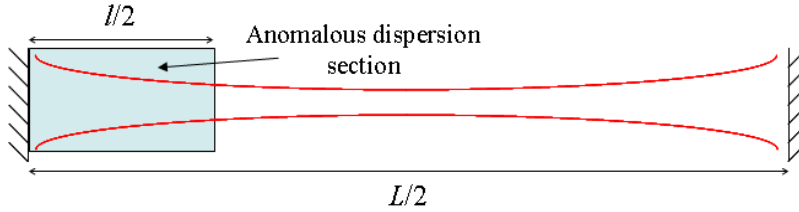


Fig. 2. An optical cavity incorporating a negative dispersion section.

The basic parameter determining the sensitivity, S , of a cavity based sensor is the ratio between the change (δL) in its effective length, and the corresponding shift ($\delta\omega$) in the resonance frequency: $S = \delta\omega/\delta L$. The larger S is, the higher the sensitivity of the sensor. For a conventional cavity, the sensitivity is given by a simple expression:

$$S = \frac{\delta\omega}{\delta L} = -\frac{n_p(\omega_{res}) \cdot \omega_{res}}{L' \cdot n_{pg}(\omega_{res})} \quad (6)$$

where n_p and n_{pg} are respectively the effective and group indices of refraction for the normal dispersive section of the cavity. For a cavity incorporating a negative slope phase component, Eq. (6) is modified, yielding:

$$S = \frac{\delta\omega}{\delta L} = -\frac{n_p(\omega_{res}) \cdot \omega_{res}}{L' \cdot n_{pg}(\omega_{res}) + c_0 \left. \frac{d\theta}{d\omega} \right|_{\omega_{res}}} \quad (7)$$

Note, that for the WLC condition Eq. (5), the sensitivity Eq. (7) approaches infinity. Nevertheless, it should be clear that in practice infinite sensitivity cannot be attained because of higher order dispersions of the cavity medium and the phase component.

3. Fiber laser implementation

The most critical issue in the “fast-light” laser is, of course, the realization of a phase component with the desired response. Such phase elements have been proposed and demonstrated using vapor cells which were optically pumped in a precise configuration.

Nevertheless, such realization is less appropriate for compact devices suitable for deployment in the field. Alternatively, the desired phase component can be realized by a Fabry-Perot or a ring resonator, as illustrated in Fig. 3.

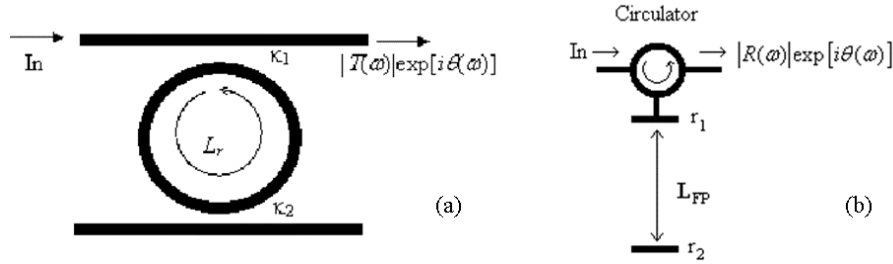


Fig. 3. (a) Ring resonator and (b) Fabry-Perot interferometer based negative dispersion components.

The maximal negative phase slope is attained at the resonant frequency of the ring satisfying $L_r k_0 n_{\text{eff}} = 2\pi m$ and Fabry-Perot satisfying $2L_{\text{FP}} k_0 n_{\text{eff}} = 2\pi m$ accordingly. The phase response of the phase element depicted in Fig. 3 is given by:

$$\tan(\theta) = -\frac{\kappa_1 \sqrt{1-\kappa_2} \sin(\phi)}{\sqrt{1-\kappa_1}(2-\kappa_2) - \sqrt{1-\kappa_2}(2-\kappa_1) \cos(\phi)} = -\frac{r_2(1-r_1^2) \sin \phi}{r_1(1+r_2^2) - r_2(1+r_1^2) \cos \phi} \quad (8)$$

where $\phi = L_r n_{\text{eff}} \omega / c = 2L_{\text{FP}} n_{\text{eff}} \omega / c$, κ_1 and κ_2 are the power coupling coefficients as shown in Fig. 3(a) and r_1 and r_2 are the mirror reflection coefficients as shown in Fig. 3(b). Both Ring Resonator and Fabry-Perot implementations are mathematically analogous with $\kappa_{1,2} = 1-r_{1,2}^2$ and $L_r = 2L_{\text{FP}}$. Equation (8) provides the phase shift introduced by the additional cavity. In order to attain a WLC, Eq. (8) must satisfy Eq. (5). Introducing the derivative of Eq. (8) with respect to the frequency at resonance into Eq. (5) provides the relations between κ_1 and κ_2 needed to achieve the WLC condition and similarly for r_1 and r_2 :

$$L' = \frac{\kappa_1 \sqrt{1-\kappa_2} L_r}{(\sqrt{1-\kappa_1} - \sqrt{1-\kappa_2})(1 - \sqrt{1-\kappa_1} \sqrt{1-\kappa_2})} = \frac{2r_2(1-r_1^2) L_{\text{FP}}}{r_1(1+r_2^2) - r_2(1+r_1^2)} \quad (9)$$

From Eq. (9) it is possible to extract a relation between κ_1 and κ_2 for a given ratio between the cavities lengths: $M = L'/L_r = L'/2L_{\text{FP}}$. Introducing $\alpha^2 = r_1 = 1-\kappa_1$ and $\beta^2 = r_2 = 1-\kappa_2$, yields the following relation between the coefficients:

$$\beta = \frac{1}{2\alpha} \left[1 + \alpha^2 - \frac{1-\alpha^2}{M} - \sqrt{(1+\alpha^2 - [1-\alpha^2]/M)^2 - 4\alpha^2} \right] \quad (10)$$

From Eq. (9) it is clear that precise control of the coupling/mirror reflection coefficients of the phase element is needed. Although such control is difficult in integrated optics, tunable fiber couplers are available and fiber Bragg grating mirrors can be tension-controlled to produce the necessary reflection coefficient. In addition, fiber optics possesses extremely low loss which is important because the phase element also introduces losses. However, a fiber based laser is inherently long, exhibiting a small free spectral range. Because of the loss associated with the phase element it is very likely that the lasing mode would not be the one satisfying the WLC but one of the “regular” modes. To overcome this problem it is necessary to provide a relatively narrow gain - at least narrower than the FSR of the main laser cavity. Because of the narrow linewidth needed, the almost obvious choice of gain process is Brillouin scattering, with gain linewidth narrower than 30MHz, and simple tunability of the peak frequency by means of strain or pump wavelength.

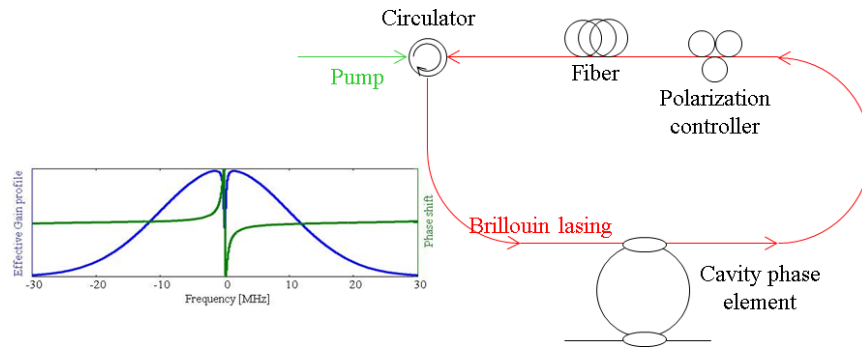


Fig. 4. Schematic of a SRS based superluminal fiber laser; Inset: effective gain and phase profiles.

Figure 4 illustrates a schematic of a superluminal Brillouin ring laser setup. The continuous wave (CW) pump beam is launched into the ring laser via a circulator, thus ensuring it would not resonate within the ring laser. For the Brillouin amplification, which occurs for a probe in the opposite direction to the pump beam, the circulator forms a closed ring cavity which can lase if the gain is sufficient. The phase element is introduced into the cavity to satisfy the WLC condition for the *lasing* frequency (not the pump). The inset shows schematically the effective gain profile and the corresponding phase profile. The additional cavity introduces a notch in the center of the Brillouin gain profile, resulting in a negatively sloped phase profile [12,14,15]

Brillouin scattering is a nonlinear process where a forward traveling electromagnetic wave interacts with the transmission medium to generate acoustic phonons and a scattered, backward traveling, electromagnetic wave. Beyond a certain threshold, the phonons interfere constructively and travel through the medium as an acoustic wave. The acoustic wave causes small periodic density variations in the medium producing a refractive index grating that further stimulates the scattering process. The backward traveling wave generated in this process of stimulated Brillouin scattering (SBS) is downshifted by $\nu_B = 2nv_a/\lambda$ compared to the frequency of the forward traveling wave (where n is the effective refractive index of the medium, ν_a is the speed of sound in the medium and λ is the vacuum wavelength of the forward traveling wave). The linewidth of the scattered wave is determined by the acoustic absorption of the medium. In optical fibers, $\nu_B \approx 10.8\text{GHz}$ while the linewidth $\Delta\nu$ ranges from 10 to 30MHz. By using a cavity with a FSR larger than $\Delta\nu$ (roughly $L' < 10.5m$) while pumping the cavity using a strong tunable laser source, in a setup similar to Fig. 4, substantial gain can be provided for the desirable WLC cavity mode, overcoming losses and favoring it from the other cavity modes. As a concrete example, consider a 10m long fiber cavity, with a roundtrip loss (due to a combination of the transmission losses from the circulator and the phase component) of approximately 1.5dB (see also section 5). Using the Brillouin gain coefficient of a single mode fiber ($\gamma = 0.14 \text{ m}^{-1}\text{W}^{-1}$ [18]), the threshold gain of a single pass comes out to be ~ 1.41 , corresponding to a pump power of $\sim 225\text{mW}$.

To achieve the optimal conditions for superluminal lasing, the resonance frequencies of both the main ring cavity and the phase element cavity are set to the peak frequency of the Brillouin gain. Because both cavities are formed by fibers, this requirement means that their circumferences must be related by a rational fraction: $L/L_r = m_1/m_2$, where m_1 and m_2 are integers. The resonance frequencies are set to the peak frequency of the gain in order to optimize the lasing conditions and avoid changes in the lasing frequency due to the Brillouin lineshape dispersion.

4. Sensitivity enhancement in Brillouin ring fiber laser

In order to evaluate the sensitivity enhancement of the fast-light laser (compared to a conventional laser) we calculated the shift in the lasing frequency due to a small modification in the main ring cavity L' . Following this modification the resonance frequency must be recalculated taking into account the dispersion of the Brillouin gain and (for the superluminal laser) the dispersion of the phase element. Designating the frequency shift in a conventional Brillouin laser by $\Delta\omega_c$ and that in a superluminal laser by $\Delta\omega_s$, we define the sensitivity enhancement as $\zeta = \Delta\omega_s/\Delta\omega_c$.

We assume that without the cavity length perturbation the superluminal laser is resonating at frequency ω_{res} satisfying:

$$\frac{\omega_{res}}{c_0} n_p(\omega_{res}) \cdot L' + \theta(\omega_{res}) = 2\pi m \quad (11)$$

When the cavity is perturbed, the new lasing frequency satisfies:

$$\frac{(\omega_{res} + \Delta\omega_s)}{c_0} n_p(\omega_{res} + \Delta\omega_s) \cdot (L' + \delta L) + \theta(\omega_{res} + \Delta\omega_s) + \Delta\theta_{Br}(\omega_{res} + \Delta\omega_s) = 2\pi m \quad (12)$$

where $\Delta\theta_{Br}$ is the phase shift caused by the dispersion of the *saturated* Brillouin lineshape. Equation (12) satisfies only the phase condition for the lasing frequency and must be supplemented by the amplitude condition. It should be noted that although the sensitivity depends on the resonance condition, the amplitude condition determines the necessary gain (pump level) for lasing which, in turn, affects the dispersion properties of the saturated gain, $\Delta\theta_{Br}$ in Eq. (12). Note, that for a conventional laser, the equations are identical except that $\theta = 0$.

To properly account for $\Delta\theta_{Br}$, it is necessary to solve for the laser threshold conditions and employ the relations between the real and imaginary part of the susceptibilities [19]:

$$\chi' = 2\chi''(\omega - \omega_0)/\Delta\omega_{Br} \quad (13)$$

where ω_0 is the frequency at which the Brillouin gain peaks (set to the resonance frequency of the WLC) and $\Delta\omega_{Br}$ is the linewidth of the Brillouin gain. χ' and χ'' are respectively the real and imaginary parts of the dielectric susceptibility. When the system is lasing, the gain compensates the overall roundtrip losses of the cavity. Denoting the roundtrip transmission as T , then χ' and χ'' are given by:

$$\begin{aligned} \chi'' &= -\ln(T)/k_0 n L_l \\ \chi' &= -2 \frac{\ln(T)}{k_0 n L_l} \frac{\omega - \omega_0}{\Delta\omega_{Br}} \end{aligned} \quad (14)$$

where k_0 and n are respectively the wavenumber and the refractive index of the fiber.

Equation (14) indicates that the dispersion of the Brillouin gain modifies the propagation coefficient in the fiber according to the following relation:

$$\Delta\beta = -k_0 n \chi' = 2 \frac{\ln(T)}{L_l} \frac{\omega - \omega_0}{\Delta\omega_{Br}} \quad (15)$$

The Brillouin gain phase shift is then given by:

$$\Delta\theta_{Br} = 2 \cdot \ln(T) \frac{\omega - \omega_0}{\Delta\omega_{Br}} \quad (16)$$

Note that because the resonance frequency of the laser is set to the gain peak, the Brillouin gain introduces a linear phase shift which for the WLC condition Eq. (5) is equivalent to a

modification of the laser roundtrip length. For example, assuming $\Delta f_{\text{Brillouin}} = 40\text{MHz}$ and $T = 0.9$, the effective additional length induced by the Brillouin phase shift is $\sim 1\text{m}$.

In order to get a broader view of the dependence of ξ on the laser parameters, we calculate the enhancement for all the combinations of κ_1 and κ_2 and for various ratios between L' and L_r (a Fabry-Perot based arrangement is completely analogous, as shown above). Figure 5 depicts the optimal relation between the coupling coefficients for L'/L_r of 1/3, 0.5, 1, 2, 3, and 4 as calculated from Eq. (12). For the simulations, the chosen parameters were $L' = 10\text{m}$, $\Delta f_{\text{Brillouin}} = 40\text{MHz}$, and “central” wavelength of $1.55\mu\text{m}$. The ring laser circumference was chosen in order to ensure a single cavity mode within the Brillouin gain line. Note that as the cavity of the phase element becomes shorter, the optimal κ_2 for a given κ_1 becomes smaller, pushing the phase element closer to the critical coupling regime. However, it should be clear that the closer the phase element cavity to critical coupling, the larger the loss induced by this element (i.e. lower T in Fig. 3).

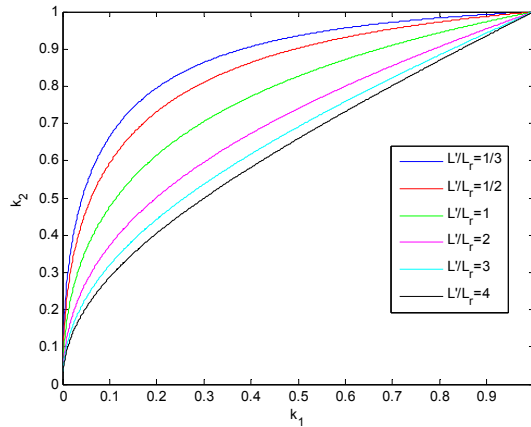


Fig. 5. Relationship between the coupling coefficients for maximal sensitivity enhancement.

The excess roundtrip loss introduced by the phase component is the transmission loss of the through port on the additional resonator, given by:

$$T(\omega_{res}) = 1 - \frac{\kappa_1^2 \kappa_2^2}{(1 - \alpha\beta)^2} \quad (17)$$

Figure 6 depicts the sensitivity enhancements and the corresponding cavity roundtrip transmission (or, equivalently, excess loss) induced by the phase component. It is clear that larger sensitivity enhancements go hand in hand with larger cavity losses. This is because higher enhancement levels require steeper phase shifts which, in turn, correspond to deeper notches in the transmission function of the phase component. The excess loss limits the minimum measurable amount of perturbation. As such, it is important to minimize this loss while maximizing the degree of enhancement. This issue is explained, and discussed in some detail, in Section 7.

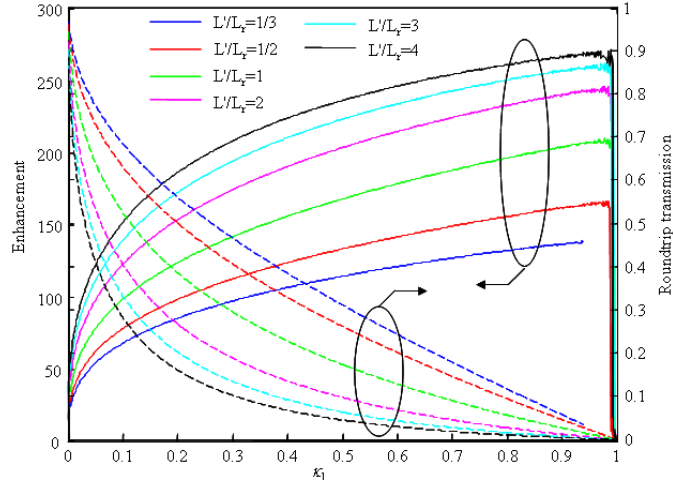


Fig. 6. Enhancement (solid) and roundtrip transmission (dashed) of superluminal lasers with optimal κ_1 and κ_2 relations for maximal enhancement.

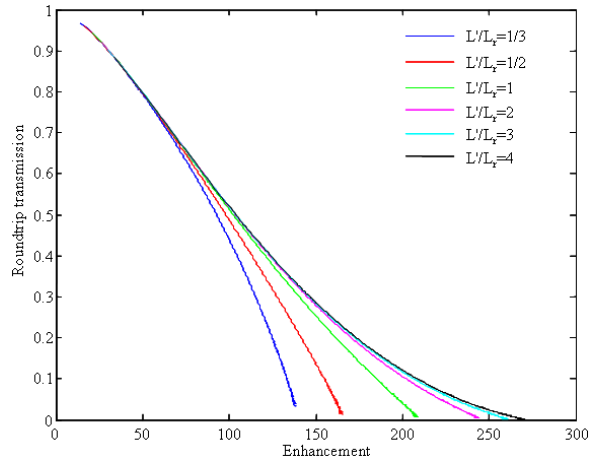


Fig. 7. Enhancement-roundtrip loss tradeoffs for superluminal laser with various cavity length ratios.

In view of Fig. 6, we note that there are many combinations of parameters which can provide any given sensitivity enhancement. Therefore, it is possible to optimize the laser and attain, for example, lower threshold levels (e.g. lower power consumption) by properly choosing the length of the cavity comprising the phase component and the coupling coefficients. It is, therefore, instructive to obtain the design curves connecting the sensitivity enhancement with the corresponding cavity roundtrip loss. Figure 7 depicts the loss-enhancement tradeoff for various cavity length ratios. Clearly, shorter phase element cavities provide smaller roundtrip losses for a given enhancement level. Nevertheless, for relatively lower enhancement levels (which correspond to lower losses), there is no real difference among the phase elements. Non-negligible loss differences are visible only for enhancement levels which exceed 70 which correspond to cavity roundtrip transmission of ~ 0.65 . Moreover, an order of magnitude improvement ($\xi \sim 15$) can be achieved with excess losses of only 3% per roundtrip, thus rendering the introduction of the additional phase component a very attractive method for achieving more sensitive sensors.

5. Nonlinearity of the sensitivity enhancement

Ideally, the sensitivity enhancement in the WLC configuration is independent of the induced change in the cavity optical length. In practice, a perfectly linear negative phase slope is difficult to achieve (particularly using an additional cavity), resulting in a satisfaction of WLC condition at a single frequency point. As a result, the enhancement of the sensitivity depends on the actual shift δL in the cavity length and is expected to decrease for larger δL . Specifically, the sensitivity enhancements depicted in Figs. 6 and 7 were found for $\delta L = 0.1\text{nm}$ but it is expected to increase for smaller changes and to decrease for larger changes.

In order to estimate the nonlinearity of the sensitivity enhancement we include the Brillouin phase shift as an additional effective length of the fiber laser. We assume the sensor and the additional cavity are designed to satisfy the WLC condition at the resonance frequency according to Eq. (9). For small changes in the cavity length we expand Eq. (12) using Eq. (8) to the third order in $\delta\omega$ and δL , yielding the following Eq. for $\delta\omega$:

$$\frac{(\omega_{res} + \delta\omega)}{c_0} (L' + \delta L) \cdot n_p + \theta(\omega_{res} + \delta\omega) = 2\pi m$$

where $\theta(\omega_{res} + \delta\omega) \approx -A\delta\omega + B\delta\omega^3$, $A = \frac{n_p L_r}{c_0} \frac{\sqrt{R_2}(1-R_1)}{(\sqrt{R_1} - \sqrt{R_2})(1 - \sqrt{R_1 R_2})}$ and (18)

$$B = \frac{(n_p L_r)^3}{c_0^3 (\sqrt{R_1} - \sqrt{R_2})} \left[\frac{\frac{1}{6} \sqrt{R_2}(1-R_1)}{(1 - \sqrt{R_1 R_2})} + \frac{\frac{1}{2} R_2(1-R_1^2)}{(\sqrt{R_1} - \sqrt{R_2})(1 - \sqrt{R_1 R_2})^2} \right] + \frac{1}{3} \frac{R_2^{\frac{3}{2}}(1-R_1)^3}{(\sqrt{R_1} - \sqrt{R_2})^2 (1 - \sqrt{R_1 R_2})^3} = \frac{(n_p L_r)^3}{c_0^3} \bar{B}$$

and we introduced $R_i = 1 - \kappa_i$. Assuming the sensor is set to the WLC Eq. (9), then Eq. (18) yields a simple cubic equation for $\delta\omega$ which can be readily solved:

$$\delta\omega = - \left(\frac{n_p \omega_{res} \cdot \delta L}{c_0 \cdot B} \right)^{1/3} \quad (19)$$

Note, that the shift in the resonance frequency is not a linear function of the cavity length change δL (the measured quantity) which means that the sensitivity enhancement is not a constant but rather depends on the measured quantity:

$$\xi = M \cdot \left(\frac{\lambda^2 / n_p^2}{4\pi^2 \cdot \bar{B} \cdot \delta L^2} \right)^{1/3} \quad (20)$$

Figure 8 illustrates an example of the sensitivity enhancement dependence on the detected quantity. The parameters of the sensor are $L'/L_r = 2$, $\kappa_1 = 0.5$ and $\kappa_2 = 0.7414$, corresponding to an optimal configuration. As shown in the figure, the sensitivity enhancement increases dramatically for small δL , exceeding 400 for $\delta L \sim 10\text{pm}$. However, the sensitivity enhancement drops rapidly as δL is increased although the enhancement for $\delta L \sim 1\text{nm}$ still exceeds 20.

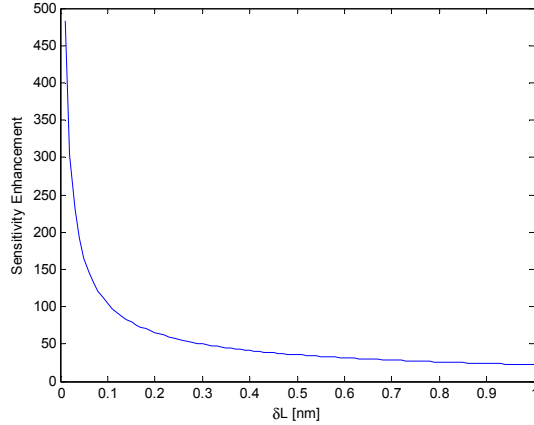


Fig. 8. Dependence of the sensitivity enhancement on δL .

6. Design tradeoffs

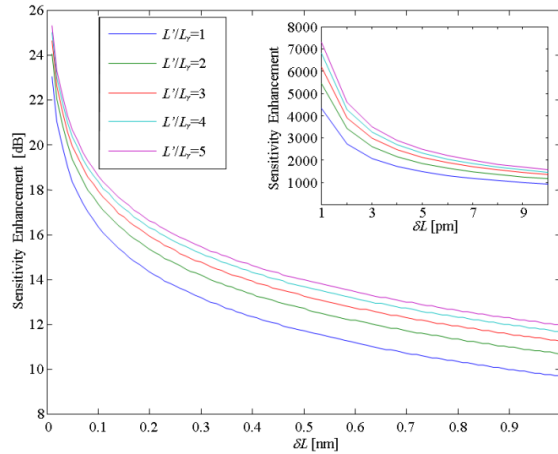


Fig. 9. Dependence of the sensitivity enhancement on the cavity length of the phase component. Inset: zoom in on smaller δL levels.

From Eq. (20) it is clear that shorter additional cavities provide larger enhancement levels, although the relation is not linear because M also affects the relations between κ_1 and κ_2 , as can be seen from Eq. (11). However, the improvement in the sensitivity enhancement is accompanied by larger excess roundtrip losses induced by the phase component. Figure 9 depicts the dependence of the sensitivity enhancement on δL for several values of M , where $\kappa_1 = 0.03$ and κ_2 for each M is found from Eq. (11). The inset zooms in on smaller δL range (in linear scale). The enhancement is shown in a logarithmic scale in order to clarify the difference between the various M levels. Figure 10 depicts the excess roundtrip losses induced by the phase component. For $M = 1$ the phase component introduces excess losses of 30% per roundtrip while for $M = 5$ the loss exceeds 50% per roundtrip. Thus, although the phase components with shorter cavities provide larger enhancement level, the substantial excess loss they induce may pose a serious problem.

Another important parameter which affects the enhancement level and the excess loss is the combination of coupling coefficients. As κ_2 is determined directly by κ_1 , it is the choice of κ_1 which eventually determines the enhancement and the excess loss. Figure 11 depicts the sensitivity enhancement as a function of δL for several coupling coefficients (κ_1). The inset depicts the corresponding excess losses. Decreasing κ_1 results in an overall lower sensitivity

enhancement factor but also lower excess losses. Therefore, Fig. 11 provides the necessary design tradeoffs allowing for optimizing and balancing between desired enhancement levels and acceptable roundtrip losses.

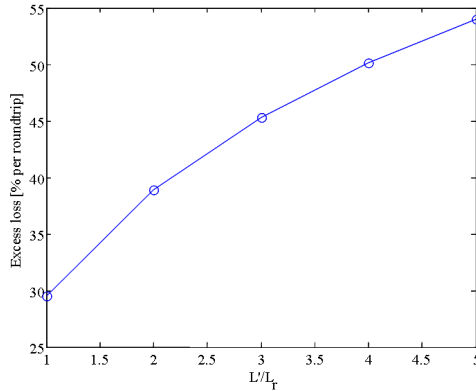


Fig. 10. Dependence of the excess roundtrip loss on the cavity length of the phase component.

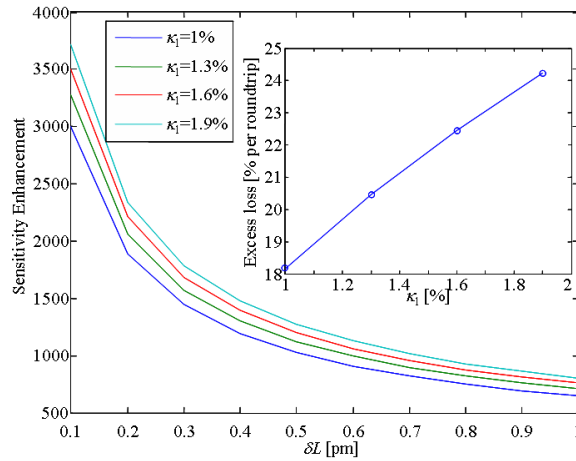


Fig. 11. Dependence of the sensitivity enhancement on the coupling coefficients. Inset: corresponding excess roundtrip losses.

7. Some practical considerations

Conceptually, the introduction of the additional phase component provides substantial enhancement in the sensitivity of the sensor. However, a practical and precise measurement of resonance frequency shifts is not trivial and requires special care. For example, it is advantageous to perform a relative frequency measurement of such shifts compared to a fixed reference frequency. In the Brillouin fiber laser implementation, such reference is readily available – the frequency of the pump laser. Beating the signal of the fiber laser with the pump laser provides a difference frequency in the range of ~ 10.8 GHz, depending on the exact resonance of the cavity. Changes in the cavity length will be accompanied by modifications of the frequency of the beat signal.

Nevertheless, one of the major problems of any optical sensor is achieving selective sensitivity, i.e. canceling the impact of other mechanisms that can modify the optical length of the laser cavity which basically act as noise sources. In a WLC based laser sensor, the sensitivity of the lasing wavelength to such, undesired, effects (e.g. vibrations, acoustic and thermal noise, etc.) is enhanced by the same amount as the sensitivity to changes in the desired property. This means that the linewidth of a WLC laser is expected to be noisier, and

hence broader, than that of a similar non-WLC laser. An appropriate approach to overcome this problem is to compare the lasing properties of the sensor to that of an identical laser located in similar environment (and experiencing the same negative dispersion) but is not subjected to the process which is being detected. Since the sensor studied here is based on a fiber ring laser, the almost straightforward method to implement such configuration is to realize an additional and similar laser which is wound on the same spool as the sensor and is not subjected to the perturbation being detected. Using heterodyne detection of the signals emerging from the fiber lasers it is possible to cancel out the common noise components, allowing for the detection of the desired signal.

The nonlinear relation between the resonance shift and the change in the cavity length causes the WLC sensor to be substantially more sensitive for smaller δL . As shown in Fig. 8, the sensitivity enhancement varies over an order of magnitude for δL ranging between 10pm to 1nm. Such nonlinear response makes it difficult to use the induced resonance shift as a direct measure to the change in the cavity length in an “open-loop” configuration. Thus, in order to take advantage of the large sensitivity enhancement at small δL , it is advantageous to operate such sensor in a “closed-loop” configuration in which a counter modification in the cavity length is introduced in order to return the resonance frequency to its “original” value.

Finally, we consider the effect of excess loss introduced by the addition of the phase component. For the configuration described above, where the signal is observed by measuring the beatnote between two nearly identical lasers, each experiencing negative dispersion, the accuracy of the frequency measurement is expected to be limited by quantum noise only. In this limit, the fluctuation in the frequency can be expressed as [20–22]:

$$\Delta\omega_{rms} = \frac{1}{Q} \left(\frac{\hbar\omega^3}{PT} \right)^{1/2} \quad (21)$$

where we have added the uncorrelated quantum noise from the two lasers. Here, P is the output power of each laser, T is the measurement time, ω is the laser frequency, and Q is the quality factor of the laser resonator:

$$Q = \omega\tau = L'\omega/c\Lambda \quad (22)$$

where τ is the lifetime of a photon in the laser cavity, and Λ is the loss per roundtrip. For example, if a roundtrip loss is 3%, we have $\Lambda = 0.03$.

The minimum measurable value of δL , which is proportional to the perturbation of interest, is a key measure of the efficacy of the sensor, is proportional to this frequency fluctuation. Explicitly, we can express this as:

$$\delta L_{min} = \frac{\Delta\omega_{rms}}{\xi S} = \frac{1}{\xi S} \cdot \frac{1}{Q} \cdot \left(\frac{\hbar\omega^3}{PT} \right)^{1/2} \quad (23)$$

where S is the sensitivity defined in Eq. (6), and ξ is the enhancement factor defined in the first paragraph of Section 4. Thus, we see that for a given sensitivity and a measurement time, the minimum measurable perturbation is proportional to $\Lambda/(\xi P^{1/2})$. For a given Brillouin pump power available, the power of the sensing laser, P , generally decreases with increasing Λ . The exact variation of P as a function of Λ depends on the nature of gain saturation. In the limit of a lasing condition where loss equals unsaturated gain, P is proportional to $1/\Lambda$. Taking this as the limiting case, we can see that the minimum measurable perturbation is proportional to (Λ^ϵ/ξ) , where the exponent ϵ has a value somewhere between 1 and 3/2. This dependence should be used as a guide in determining the optimal operating condition for the sensor. Of course, we must also ensure that the loss is small enough so that the available pump power is above the lasing threshold. Note that in Eq. (23) the sensitivity enhancement parameter, ξ , itself

depends on δL . Specifically, ζ increases with decreasing δL . Thus, Eq. (23) has to be solved in a self-consistent manner. Numerically, this can be done by evaluating the right hand side (RHS) of Eq. (23) for decreasing values of δL until it (the RHS) matches the value of δL .

As an example, we calculate δL_{\min} for a 1 m WLC fiber laser with intrinsic losses of 5% per revolution where the pump is set to attain a value of $P = 10\text{mW}$ inside the cavity in the absence of the additional phase component. Figure 12 shows δL_{\min} as a function of κ_1 for a WLC laser where $M = 1$ and κ_2 is set to meet the WLC condition. For comparison, δL_{\min} for a conventional fiber laser with the same length and 1 sec averaging time is $\sim 4.4 \times 10^{-17}\text{m}$. As can be seen, the minimal measurable δL_{\min} is smaller by nearly 8 orders of magnitudes for a relatively large range of coupling coefficients κ_1 . This is a highly attractive property because it means that the precise values of parameters are relatively unimportant as long as the laser lases and the WLC is satisfied.

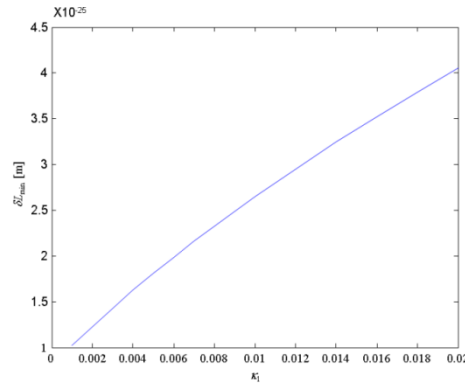


Fig. 12. Dependence of the δL_{\min} on the coupling coefficient κ_1

Several additional issues must also be considered in the design of the laser. First, nonlinear effects (Kerr, Raman, four wave mixing, etc.) might modify the properties of the laser. However, because the cavity is short (10m), the finesse is relatively low and the lasing power in the cavity is modest ($F \sim 10$ and $P = 10\text{mW}$ in the above example), the impacts of the Kerr effect and Raman scattering are not expected to impair significantly the performance of the sensor, as discussed below. Four wave mixing process is also inefficient because the pump and signal are counter-propagating and the pump is not resonant in the cavity (single pass). Second, control of polarization is also required in order to ensure single mode operation. This can be done either by introducing a polarization controller to the cavity (as in Fig. 4) or by using a polarization maintaining fiber. Finally, Rayleigh scattering in the lasing frequency cannot build up because of the circulator located in the cavity forcing uni-directional lasing.

It should be emphasized that each of these effects produces a constant bias (e.g. a constant shift in the resonance frequency due to the Kerr effect) as well as fluctuations. A constant bias can be taken into account, and plays no role in limiting the sensing ability of the proposed device. On the other hand, the fluctuation, due in turn to random variation in the relevant parameters, is equivalent to noise, which may limit the minimum measurable perturbation. As a general rule, in order for the sensor to reach its optimal sensitivity it is necessary to suppress all classical noise sources, including those due to fluctuations in nonlinear effects, below the quantum noise limit, by careful control of the system. As an example, let us consider the impact of power fluctuations through the Kerr effect. The highest optical power in the scheme is that of the pump, which should be of the order of $\sim 200\text{mW}$. Based on the nonlinear refractive index and the effective area of single mode fibers [23], reducing the frequency fluctuations due to intensity noise below the quantum limit, as given by Eq. (21) above, requires the pump fluctuations to be below 2mW. Thus, the pump intensity should be

stabilized to a level of ~1% which is very easy to achieve. Similar conclusions apply to the other nonlinear effects mentioned above. Thus, these non-idealities are unlikely to have a major impact on the measuring abilities of the proposed scheme.

8. Conclusions

“Fast-light” based lasers can provide an excellent platform for enhancing the sensitivity of optical sensors. We show that the sensitivity of Brillouin laser sensors can be increased very significantly by inserting a cavity based phase element in the laser cavity. Higher enhancement levels are correlated with larger cavity roundtrip losses, which might increase the minimum measurable δL . Nevertheless, we find that because of the rapid increase in sensitivity enhancement for small cavity length perturbation, δL_{\min} can be reduced by as much as eight orders of magnitudes compared to that of conventional laser sensors for a wide range of parameters (such as loss level) as long as lasing is attained.

We study the dependence of the enhancement level on the detected quantity and find that it is highly nonlinear. The sensitivity is large for small δL and decreases rapidly when δL is increased. This property of the WLC laser stems from the fact that the phase response of the additional cavity is nonlinear and, therefore, can set the laser to the WLC condition only at a single frequency. In the study presented here, the resonance frequency of the cavity comprising the phase component is set to that of the main cavity in order to attain maximal sensitivity enhancement. Nonetheless, it is possible to detune the resonance of the phase component from that of the main cavity and attain broader enhancement (in terms of δL) for lower peak enhancement level. These and related variants of the proposed scheme will be investigated further in the future.

We also study the impact of the various parameters of the phase component on the achievable sensitivity enhancement. A clear tradeoff, which can be regarded as a general rule, is that larger enhancement level (for a given δL) is accompanied by larger roundtrip loss. This relation is important because larger losses are expected to increase the minimal measurable δL . The overall sensitivity enhancement and excess losses are determined by phase component coupling coefficients and cavity length. Larger coupling coefficients provide higher enhancement factors but also larger excess losses. The length of the phase component cavity is also important: shorter cavities can provide larger sensitivity enhancements which are, again, accompanied by higher losses. Nevertheless, the impact on the minimal measurable perturbation is relatively small because of the large enhancement levels at small perturbations.

An experimental demonstration of the proposed scheme, utilizing a non-resonantly pumped 10.5m long Brillouin laser and an equally long additional cavity which is connected to the main cavity with tunable coupler is currently in progress. Such WLC based laser sensor can potentially exhibit substantially higher sensitivity than conventional laser sensors. The solid-state, fiber optics based implementation thereof, with a narrow linewidth Brillouin gain, provides a robust and light-weight system which is convenient for field deployment.

Acknowledgment

J. S. thanks Luc Thévenaz for stimulating discussions and useful comments. This work was supported in part by the ISF, the Israeli DoD, the US AFOSR Grant # FA9550-10-01-0228 and the exchange Program of the NU-TAU institutes for Nanotechnology supported in part by NSF award EEC- 0647560.